International Journal of Modern Physics B
Vol. 36, No. 4 (2022) 2250038 (8 pages)
© World Scientific Publishing Company
DOI: 10.1142/S0217979222500382

Constructing thermal phonon insulators by using photonic crystals

Azka Umar*,‡, Guangqiang He*, Chun Wang† and Chun Jiang*,§

*State Key Laboratory of Advanced Optical Communication System and Networks Shanghai Jiaotong University, Shanghai 200240, P. R. China

†Center for Optics Research and Engineering of Shandong University, 72 Binhai Road, Jimo Qingdao, P. R. China

‡azka_umar@sjtu.edu.cn

§cjiang@sjtu.edu.cn

Received 7 November 2021
Revised 19 December 2021
Accepted 23 December 2021
Published 14 February 2022

This paper designs a thermal waveguide using thermal phonon insulators, to manipulate the loss of thermal radiation. Two-dimensional (2D) photonic crystals with dielectric background and air holes have been used in the waveguide clad to suppress thermal radiation so that thermal radiation cannot escape out from the waveguide clad. The photonic crystals may reduce the loss of thermal radiation through waveguide clad which surges the thermal energy confinement in the waveguide core and propagation along the longitudinal axis. The photonic crystals have been designed with the bandgap covering the thermal phonon frequency range and thus can be used to construct thermal phonon insulators to suppress or trap thermal emission generated through phonon wave propagation. The finite-difference-time-domain simulation results demonstrate that electromagnetic bandgap in photonic crystals has enough width in the thermal phonon frequency range to confine the thermal energy within the core of the waveguide and effective transmission of thermal radiation can be conquered within the waveguide core.

Keywords: Phonons; photonic crystals; thermal radiation; waveguide; electromagnetic waves.

PACS numbers: 71.36.+c, 42.70.Qs, 44.40.+a, 41.20.Jb

1. Introduction

Thermal emission is a pervasive feature of nature as any object at a finite temperature emits thermal energy in the form of electromagnetic radiation with the speed of light in all directions due to thermally induced vibration of particles and quasiparticles. The ability to manipulate the flow of thermal emission is critical for

§Corresponding author.

a range of optical, electronic and thermal devices.[1] Efforts have been devoted to artificially controlling thermal radiation through the presence of bandgaps within periodic photonic and phononic materials, which is difficult to achieve with natural materials.

Photonic crystals are used to create an artificially engineered periodic dielectric material that exhibits forbidden and permitted spectral regions for electromagnetic radiation in its density of states (DOSs) spectrum.[2,3] Enlargement of these photonic bandgaps has attracted much attention, as suppression and enhancement of electromagnetic radiation are crucial optical procedures that rule the performance of infrared thermal images, detectors, thermo-photovoltaic cells, lasers and solar cells.[4–9] Another astonishing usage of the engineering photonic bandgap is the manipulation of spontaneous emission.[10] Photonic crystals are widely being used to control thermal radiations in planned electromagnetic environments provided through photonic bandgap effects because thermal emission is also a type of thermally compelled spontaneous emission, thermally equilibrium with its environs.[11–16]

Phonon is the mechanical vibration of atoms in solids and is accountable for the transmission of sound and heat energy within solids. Phonons at high frequency take the form of heat, referred as thermal phonons and these frequency thermal phonons are accountable for the major source of thermal energy transport within solids.[17] Phononic crystals are used to manipulate the transmission of sound and heat with the help of bandgap structures in its spectrum similar to the control of electromagnetic radiation by photonic crystals.[18,19] The collaboration between photons and phonons has been a topic of interest for a long time; the main goal of this combination is to increase the probability of restricting simultaneously optical and elastic waves in waveguides and cavities by manipulating the photonic and phononic band structures of those cavities and waveguides.[20–22] The accomplishment of this goal demands conquering various challenges in nanofabrication, elastic and electromagnetic wave manipulation.[23,24]

This paper focuses on the manipulation of thermal radiation generated due to electromagnetic and elastic waves within the electromagnetic stop bands of designed dielectric periodic photonic crystal waveguides. The designed thermal waveguide is composed of periodic dielectric material with air holes as a waveguide clad which have enough electromagnetic bandgap at a maximal phonon frequency range which ranges from 10 THz to 30 THz, to trap thermal radiation generated through photons and phonons within the forbidden gaps of periodic dielectric material.[25] In the proposed model, the electromagnetic thermal wave generated through thermal emission source collides with the cladding of waveguide and creates molecular vibration. By engineering the photon spectrum within its bandgap region, we can increase the flow of thermal radiation propagation generated through thermal phonon and photons within the waveguide core and the designed periodic dielectric material with air-holes that act as heat-proofing to restrict the transmission of thermal emissions within the waveguide core.

2. Theoretical Consideration

In this paper, we design a two-dimensional (2D) waveguide for thermal energy transmission, consisting of a 2 μm wide round cavity having a heating source that emits electromagnetic thermal radiations within the waveguide core at ultra-high maximal phonon frequencies. Thermal radiations interact with waveguide clad and produce thermally driven molecular vibration with the waveguide clad composed of carefully designed periodic dielectric structure with air holes. The periodic dielectric structure in the waveguide clad is composed of silicon as a constituent material with a 0.3 μm air-holes' radius as the scattering material to assemble a triangular lattice of periodic dielectric structure. Periodic dielectric structure has been used as a waveguide clad because these crystals can manipulate electromagnetic thermal emission produced due to phonon and photon wave propagation at maximal phonon frequency ranges due to the presence of energy bands in its density of state DOS spectrum.[26,27]

The designed 2D waveguide clad is periodic in two directions and homogenous in the third direction, so the harmonic modes here can be separated into two self-governing polarizations; transverse-electric TE mode and transverse-magnetic TE each with its own band structure, as we need a complete bandgap for all polarizations to simultaneously prohibit the electromagnetic waves through those bandgaps' structures. With the intention to find complete bandgaps for all polarizations in the designed periodic dielectric structure in waveguide clad, we put a triangular lattice of low dielectric columns (air holes) inside a medium with high dielectric constant (silicon); the air gaps between columns will look like localized regions of the high dielectric substrate presented in Fig. 1(a).

Figures 1(b) and 1(c) illustrate the lattice and reciprocal lattice and its irreducible Brillouin zone (IBZ) whose corners are conventionally called T, M and K for this lattice. In a triangular lattice, the choice of primitive lattice vector (R_{12}) in real space determines its reciprocal lattice vector (G_{12}) in reciprocal space in which the triangular (hexagonal) lattice governs the periodicity of the structure,

$$R_{12} = \left(\frac{\sqrt{3}}{2}, \pm\frac{1}{2}\right) a,$$

$$G_{12} = \left(\frac{1}{\sqrt{3}}, \pm 1\right) \frac{2\pi}{a}.$$

We choose the k-points along the edges of IBZ based on reciprocal lattice vector G_{12}. The k-points specify the k vectors for which we compute the band structure $\omega(k)$. The resultant band structure obtained from this configuration has a photonic bandgap for both TE and TM polarizations at ultra-high frequency ranges.[28]

2D band structure consisting of a triangular array of low dielectric cylinders within a high dielectric constant substrate is calculated with the Bloch boundary condition and eigenvalue analysis.[29]

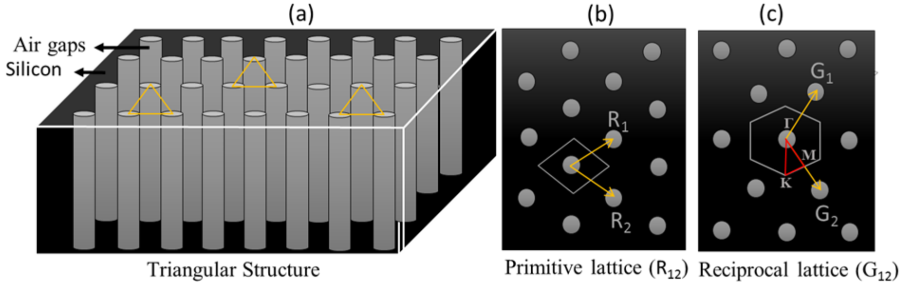

Fig. 1. (Color online) (a) The structure of the 2D photonic crystal clad of the thermal waveguide. (b) Primitive lattice (real space) and (c) Reciprocal lattice (reciprocal space).

At any finite temperature inside a body, thermal agitations cause disordered movement of charged particles and the haphazard fluctuations of those charges in return create a fluctuating electromagnetic field termed thermal radiation field as it instigates from random thermal motion.[30] The thermal emission source inside the waveguide cavity is modeled through harmonic polarization reaction P toward applied electric field E. Calculation of thermal emissions inside the waveguide core is performed under the statement of fluctuation–dissipation theorem through direct thermal radiation emission calculations,[31,32]

$$\frac{d^2P}{dt^2} + \beta\frac{dP}{dt} + \omega^2 x = \sigma E,$$

where P is the polarization response which is equal to number density n and the particles carrying charge for the polarization retort er, β indicates the system losses, ω represents the frequency of specific polarization and $\sigma = ne^2/m$, where m indicates the mass and E is the applied electric field. To model electromagnetic thermal emission, the Finite Difference Time Domain (FDTD) technique has been used under the theory of Langevin approach to Brownian motion of particles in a field of force.[33,34] Langevin equation adds a random number $K(t)$ in the presence of the applied electric field, which represents the presence of thermal fluctuations on the electromagnetic field in the above equation,

$$\frac{d^2P}{dt^2} + \beta\frac{dP}{dt} + \omega^2 x = \sigma E + K(t),$$

where $K(t)$ in the above equation simulates the white noise spectrum in the model which corresponds to the conventional high-temperature factor in FDTD, to mimic thermal emissions and the existence of forbidden gaps in the clad of the waveguide has been used to manipulate thermal emissions to escape out of the waveguide.

3. Results and Discussion

Figure 2(a) represents the schematic diagram of 2D photonic crystals. The composition of periodic dielectric structure consists of silicon as a constituent material with a lattice constant of 1 μm and air-holes' radius of 0.3 μm which act as scattering

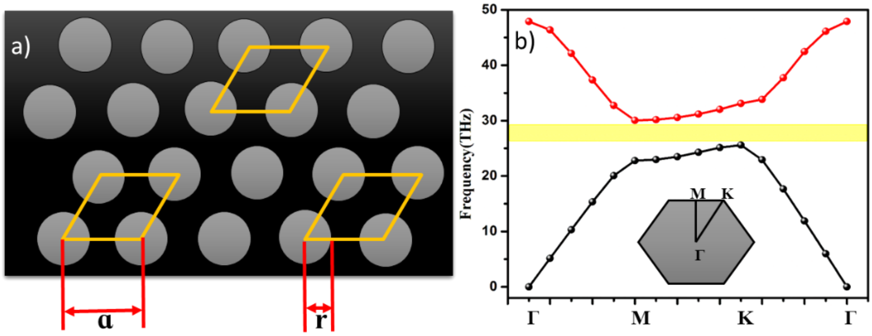

Fig. 2. (Color online) (a) 2D photonic crystals of air columns in a dielectric substrate with radius r and lattice constant a. (b) Photonic band structure of the modes spanning IBZ; yellow area shows the bandgap.

material to create a triangular lattice of periodic dielectric structure. The designed 2D photonic crystals have been used to surround a 2 μm thick microcavity which emits electromagnetic thermal radiations in all directions.

Various techniques have been used for bandgap maximization with different structural configurations[4,6]; here we use triangular lattice of low dielectric constant cylinders inside a material with high dielectric constant to obtain a full and wide bandgap at ultra-high frequencies positioning within the maximal phonon frequency ranges. By defining the primitive lattice vector R_{12} and obtaining its reciprocal lattice vectors G_{12}, we apply periodic boundary conditions with subsequent Maxwell equations by confining the eigenvalue problem to the photonic crystal unit cell and acquire the band structure of our 2D model along the edges of IBZ which has enough electromagnetic bandgap to trap thermal radiations, as shown in Fig. 2(b). The results show that with the designed 2D configuration a wide bandgap appears at the frequency range of 27–30 THz for both TE and TM polarities, which takes the form of thermal phonon insulators as the frequency range includes the maximal phonon frequency range and can help in improving the flow of thermal radiation propagation generated through thermal phonon and photons within the waveguide core.

After cautiously scheming the triangular array of air holes in 2D photonic crystals which results in enough electromagnetic bandgap within the thermal phonon frequency range of 27–30 THz, we design a thermal waveguide by using our designed 2D photonic crystals as a clad to trap thermal radiations produced due to photon and phonon within its bandgap structures within the same frequency range.

Figure 3(a) shows the schematic diagram of a 2D thermal waveguide with a 2 μm wide core surrounded by a 2D periodic dielectric material with a triangular array of air columns. Waveguide core contains thermal emission source modeled by using the theory of Langevin approach to Brownian motion of a particle in a field of force, which emits thermal radiation in all directions within the waveguide and the designed periodic triangular procedure of air holes in a dielectric substrate is used

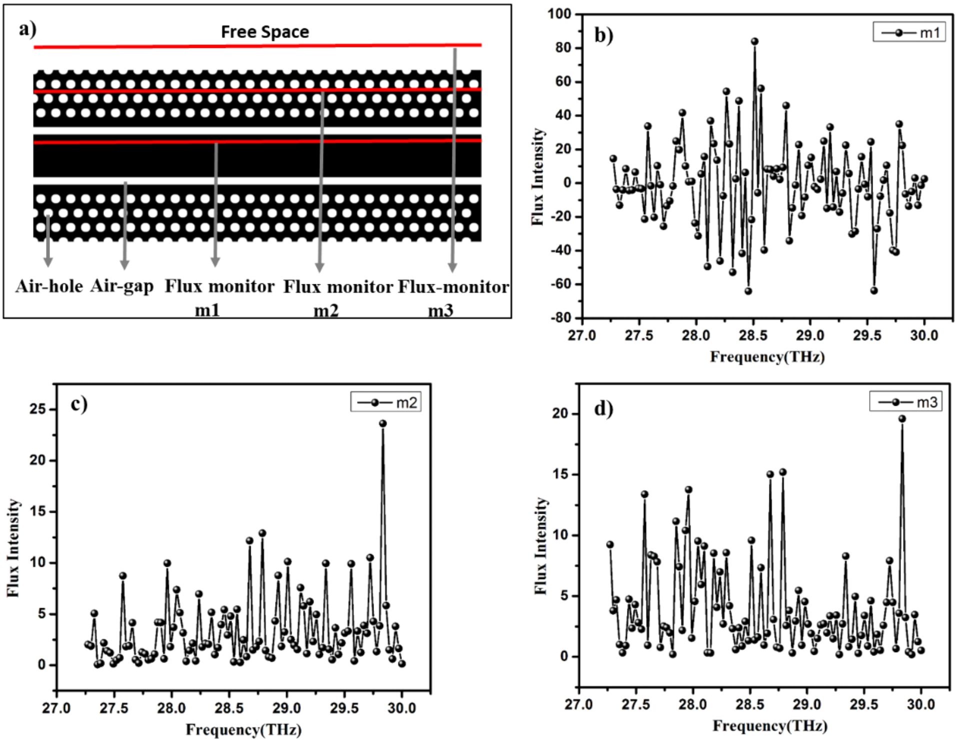

Fig. 3. (Color online) (a) Schematic diagram of 2D thermal waveguide with a microcavity surrounded by dielectric substrate with a triangular array of air columns and the flux monitors m1, m2 and m3. (b) Flux spectra of flux monitor m1. (c) Flux spectra of flux monitor m2. (d) Flux spectra of flux monitor m3.

as heat-proofing for thermal radiations so that heat energy can be confined within the waveguide core. To measure the intensity of thermal radiations, thermal flux monitors have been positioned at three limited places in the designed waveguide: one situated inside the cavity to quantify the concentration of thermal emission inside the core cavity and the other one around the core in designed 2D photonic crystals clad and the third one in free space around the waveguide.

Figure 3(b) demonstrates the flux strength of the monitor located at the flux monitor m1 which is inside the core of the waveguide within the frequency range of 27–30 THz with the highest flux intensity of 90 on 28 THz frequency, which is the highest gain of the intended thermal waveguide. Figure 3(c) illustrates the flux strength of monitor sited at flux monitor m2 positioned within the clad of the thermal waveguide; the intensity of thermal flux drops to the maximum highest peak of 25 inside our designed triangular array of air holes in the dielectric substrate due to the presence of forbidden gaps. Figure 3(c) shows the flux intensity of the flux monitor m3 placed outside the waveguide in free space, with a further reduction of thermal flux to 18.

The simulation results prove that by finding bandgap frequencies of 2D photonic crystals assembled through a triangular array of air holes in dielectric materials and manipulating high-temperature modes through bandgap structures, the proposed model of thermal radiation control through thermal phonon insulators can increase the thermal emission propagation within the waveguide core and heat energy is not allowed to escape out of the waveguide clad.

4. Conclusion

In this paper, we design thermal phonon insulators by using a periodic dielectric structure with air-holes as a clad which have sufficient electromagnetic bandgap to restrict thermal radiations generated through the photons and phonons within a thermal waveguide core. A radiating heat source has been modeled under the theory of Langevin approach to Brownian motion of a particle in the applied electric field within the core of the waveguide, which collides with the waveguide clad and creates molecular vibration within the waveguide core. Simulation results prove that the designed periodic dielectric structure can act as thermal phonon insulators at maximal phonon frequency range as it has enough electromagnetic bandgap to manipulate thermal radiations generated through phonons and photons within their stopbands. Our designed model can boost thermal radiations within the waveguide core and heat is not allowed to escape out of the waveguide through the designed thermal phonon insulators, which may offer prospects for applications that implicate the spectral control of radiation management at ultra-high frequencies.

Acknowledgments

This work was financially supported by the Key-Area Research and Development Program of Guangdong Province under Grant No. 2018B030325002 and the National Natural Science Foundation of China (Grant Nos. 61975119 and 62075129).

References

1. B. Zhao *et al.*, *ACS Photon.* **8**, 872 (2021).
2. C. M. Cornelius and J. P. Dowling, *Phys. Rev. A* **59**, 4736 (1999).
3. Y. Gong *et al.*, *Nanophotonics* **10**, 1285 (2021).
4. M. Maldovan, W. C. Carter and E. L. Thomas, *Appl. Phys. Lett.* **83**, 5172 (2003).
5. C.-J. Wu, Y.-N. Rau and W.-H. Han, *Prog. Electromagn. Res.* **100**, 27 (2010).
6. D. Wan and S. C. Glotzer, *Phys. Rev. Lett.* **126**, 208002 (2021).
7. R. K. Cersonsky *et al.*, *Nat. Commun.* **12**, 1 (2021).
8. A. Lenert *et al.*, *Nat. Nanotechnol.* **9**, 126 (2014).
9. T. Inoue *et al.*, *Opt. Exp.* **26**, A192 (2018).
10. E. Yablonovitch, *Phys. Rev. Lett.* **58**, 2059 (1987).
11. Y. Wu, X. Chen and W. Lu, *Int. J. Infrared Millimeter Waves* **27**, 425 (2006).
12. S.-Y. Lin *et al.*, *Phys. Rev. B* **62**, R2243 (2000).
13. R.-J. Shiue *et al.*, *Nat. Commun.* **10**, 1 (2019).

14. T. Inoue, T. Asano and S. Noda, *Opt. Exp.* **26**, 32074 (2018).
15. S.-Y. Lin *et al.*, *Sci. Rep.* **10**, 1 (2020).
16. W. Li and S. Fan, *Opt. Exp.* **26**, 15995 (2018).
17. M. Maldovan, *Nature* **503**, 209 (2013).
18. M. Maldovan, *Phys. Rev. Lett.* **110**, 025902 (2013).
19. T. Vasileiadis *et al.*, *J. Appl. Phys.* **129**, 160901 (2021).
20. J.-B. Béguin *et al.*, *Proc. Natl. Acad. Sci.* **117**, 29422 (2020).
21. V. Laude, Photon and acoustic phonon coupling in phoxonic crystals, in *Proc. Photonic Crystal Materials and Devices X* (International Society for Optics and Photonics, 2012), p. 84250K.
22. T. Ueta, Photon-Phonon Interaction in Photonic Crystals, in *IOP Conference Series: Materials Science and Engineering* (IOP Publishing, 2010), p. 012103.
23. M. Maldovan and E. L. Thomas, *Appl. Phys. Lett.* **88**, 251907 (2006).
24. A. Khelif *et al.*, *J. Appl. Phys.* **94**, 7944 (2003).
25. F. Bassani, G. Leidl and P. Wyder, *Encyclopedia of Condensed Matter Physics*, 1st edn. (Academic Press, 2006).
26. M. Florescu, K. Busch and J. P. Dowling, *Phys. Rev. B* **75**, 201101 (2007).
27. M. Florescu and K. Busch, *J. Opt. A. Pure Appl. Opt.* **11**, 114005 (2009).
28. J. D. Joannopoulos *et al.*, *Molding the Flow of Light* (Princeton University Press, Princeton, NJ, 2008).
29. S. G. Johnson and J. D. Joannopoulos, *Opt. Exp.* **8**, 173 (2001).
30. J. R. Howell *et al.*, *Thermal Radiation Heat Transfer* (CRC Press, 2020).
31. C. Luo *et al.*, *Phys. Rev. Lett.* **93**, 213905 (2004).
32. A. F. Oskooi *et al.*, *Comput. Phys. Commun.* **181**, 687 (2010).
33. T. Asano *et al.*, *Opt. Exp.* **17**, 19190 (2009).
34. S. Chandrasekhar, *Rev. Mod. Phys.* **15**, 1 (1943).